ACS Catalysis

Research Article

pubs.acs.org/acscatalysis

Direct Evidence of Surface Oxidation of Cobalt Nanoparticles in Alumina-Supported Catalysts for Fischer–Tropsch Synthesis

Christine Lancelot,[†] Vitaly V. Ordomsky,[†] Odile Stéphan,[‡] Majid Sadeqzadeh,[†] Héline Karaca,[†] Maxime Lacroix,[§] Daniel Curulla-Ferré,[§] Francis Luck,[§] Pascal Fongarland,[†,∥] Anne Griboval-Constant,[†] and Andrei Y. Khodakov*[,†]

[†]Unité de Catalyse et de Chimie du Solide, UMR 8181 CNRS, Bât. C3, Université Lille 1, ENSCL, Ecole Centrale de Lille, 59655 Villeneuve d'Ascq, France

[‡]Laboratoire de Physique des Solides, Université Paris-Sud, Orsay Cedex 91405, France

[§]Total S.A., 2 Place Jean Millier, 92078 Paris la Défense France

Supporting Information

ABSTRACT: Activity and stability of cobalt nanoparticles supported on mesoporous oxides is of extreme importance for the design of efficient catalysts for low-temperature Fischer–Tropsch synthesis. Catalyst deactivation is a major challenge of this reaction. The identification of mechanisms of catalyst deactivation is indispensable for optimizing the catalyst lifetime and hydrocarbon productivity. Most of the previous reports have addressed the modification of the bulk catalyst structure during Fischer–Tropsch synthesis. The present paper provides the first direct experimental evidence of surface oxidation of supported cobalt metal nanoparticles in the Fischer–Tropsch reaction. In addition to other deactivation phenomena, the uncovered surface oxidation of cobalt nanoparticles is likely to be a major reason for catalyst deactivation at higher reaction temperatures and carbon monoxide conversions.

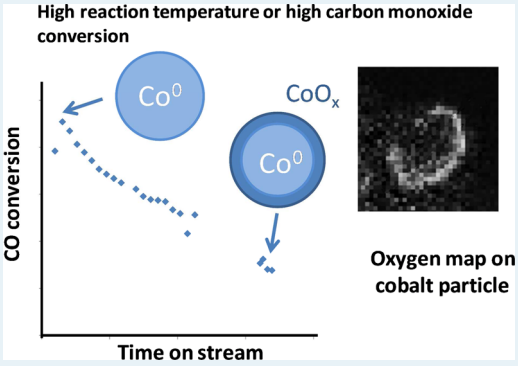

KEYWORDS: *Fischer–Tropsch synthesis, cobalt nanoparticles, catalyst deactivation, oxidation, STEM-EELS*

INTRODUCTION

Deactivation at the nanoscale level is a major challenge for catalyst design for many important catalytic reactions. Fischer–Tropsch (FT) synthesis is an efficient way of syngas (H_2/CO mixtures) conversion into liquid hydrocarbons and oxygenates, which can be produced from biomass, coal, natural or shale gas.[1−5] FT synthesis is an exothermic reaction. Low-temperature FT synthesis is typically conducted at 210–240 °C, total pressure of 20 bar, and stoichiometric H_2/CO ratio of 2 using cobalt or iron catalysts. In cobalt catalysts, the FT reaction occurs on small metal nanoparticles (6–30 nm) supported on mesoporous supports, for example, refractory oxides or carbon materials.[1−7] For the nanoparticles larger than 6–8 nm,[6] the reaction rate is proportional to the number of exposed cobalt metal surface sites.

Catalyst deactivation is a major reason for activity loss in FT synthesis. The deactivation phenomena have been recently reviewed by Saib[8] and Tsakoumis.[9] The literature suggests that major mechanisms of catalyst deactivation may involve sintering of cobalt nanoparticles, cobalt oxidation, and carbon deposition in addition to other phenomena (poisoning, cobalt restructuring, formation of mixed Co–Al oxides in the presence of large amounts of water....). Cobalt sintering at both nano- and microscopic scales, which leads to larger cobalt nanoparticles and agglomerates, has been reported using transmission,[8] scanning electron microscopies[10] and operando XRD under realistic conditions of FT synthesis.[11] Carbon deposition on alumina-supported cobalt catalysts has been recently investigated by Moodley[12] and Peña[13,14] using a combination of characterization techniques. It has been suggested that cobalt sintering principally occurs during the initial reaction period, while carbon deposition proceeds at longer time-on-stream and leads to several adsorbed carbon species.

The literature exhibits considerable controversy over oxidation of cobalt nanoparticles by water during FT synthesis, which has been evoked for a long time as one of the reasons for the deactivation of cobalt FT catalysts .[15,16] Cobalt oxidation phenomena occurring with the promoted FT catalysts have been recently reviewed by Jacobs[16,17] et al. Cobalt oxidation in K-promoted cobalt catalysts was observed by Huffman[18] et al. using in situ XANES. The changes in cobalt oxidation state often result in the modification of selectivity patterns. Ma[19] et al. investigated the influence of carbon monoxide conversion on the structure and performance of Ru-promoted Co/A_2O_3 catalyst in a slurry reactor. Much higher CO_2 and methane selectivities were observed at higher carbon monoxide

Received: July 10, 2014
Revised: October 31, 2014
Published: November 4, 2014

   dx.doi.org/10.1021/cs500981p | ACS Catal. 2014, 4, 4510–4515

conversions. The observed phenomena were attributed to the oxidation with water of metallic cobalt to CoO which catalyzes the water gas shift reaction. Azzam[20] et al. observed very rapid oxidation of ultrasmall cobalt metal particles in the KL zeolite after exposure to the FT reaction conditions. A spectacular increase in methane selectivity was observed. Partial reoxidation of cobalt particles was reported by Jermwongratanachai[21] et al. at carbon monoxide conversion of 50%. Van Steen[22] and Swart,[8] however, ruled out cobalt bulk oxidation as a possible reason for catalyst deactivation under realistic reaction conditions. Indeed, their thermodynamic calculations exclude any major bulk oxidation of cobalt metallic nanoparticles larger than 2−6 nm in FT reaction. Moreover, a gradual reduction of residual cobalt oxide particles was observed in a few reports[8,11,23,24] during FT reaction. Our combined in operando XRD/XAS investigations[11,25] also did not reveal any noticeable bulk oxidation of cobalt nanoparticles of 6−8 nm in Pt-promoted cobalt catalysts at a wide range of FT reaction conditions. Recently Fischer[26] using in situ XRD and magnetic method observed bulk oxidation of very small cobalt metal particles (∼4 nm) in FT catalysts in the presence of water, while larger cobalt particles were stable under the same conditions. The prevailing cobalt catalyst deactivation mechanism can therefore be a function of the reaction conditions. The discrepancy relevant to the oxidation of cobalt nanoparticles in FT synthesis can be also due to the lack of direct catalyst characterization techniques.

Catalysis is a surface phenomenon. Although catalyst bulk structure is essential for catalyst design, the reaction rate is principally affected by the number and intrinsic activity of the sites present on the catalyst surface. The thermodynamic properties and structure of the surface of metal nanoparticles may differ from bulk metal. Thermodynamic calculations performed in our recent report[27] predict surface oxidation of cobalt nanoparticles in the presence of very small amounts of water in hydrogen. Very little experimental information has been available so far about the evolution of catalyst surface in FT reacting medium. Indeed, most of the ex situ, in situ, and operando techniques, which have been previously used to study deactivation of FT catalysts are not selectively sensitive to the surface of metal nanoparticles.

High-resolution nanoscale imaging of supported nanoparticles is a great challenge in catalysis.[3,7] Scanning transmission electron microscopy combined with spatially resolved electron energy loss spectroscopy (STEM-EELS) is a powerful technique[3,28] for catalyst characterization at nanometer scale and provides spatially resolved information on the chemical and structural properties of the solids. In addition to chemical mapping, this technique yields important information about electronic structure such as valence state of atoms. In the past, STEM-EELS has been successfully used for characterization of several FT catalysts.[29−33] In EELS, the L ionization edges of transition metals usually display sharp peaks at the near-edge region, which are also called white lines.[34,35] The oxygen K peaks[35] can provide a fingerprint about the presence of cobalt oxide species in the catalyst and particularly can be helpful for distinguishing oxygen atoms of cobalt oxides from those of alumina support. Both CoO and Co_3O_4 display a sharp oxygen K pre-edge feature, while this feature is not present in the spectra of oxygen atoms in alumina.[30,36]

The present paper focuses on the influence of FT reaction on the structure of cobalt nanoparticles in alumina-supported cobalt catalysts using STEM-EELS. In particular, the paper addresses the phenomena which occur on the catalyst surface under different FT reaction conditions.

EXPERIMENTAL SECTION

The $CoPt/Al_2O_3$ catalyst was synthesized via incipient wetness coimpregnation using aqueous solutions of cobalt nitrate ($Co(NO_3)_2$ $6H_2O$) and tetramine platinum nitrate ($Pt(NH_3)_4(NO_3)_2$) followed by drying and calcination.[11] The cobalt and platinum contents in the catalysts were, respectively, 25 and 0.1 wt %. Before the reaction the catalyst was reduced in situ in a flow of hydrogen during 4 h at 400 °C (temperature ramping rate of 3°/min). The catalytic experiments were conducted in a millifixed bed reactor[37] with internal diameter of 2 mm. After the reduction, the catalyst was cooled to 180 °C and filled with syngas. Then the reactor pressure was increased from atmospheric to 20 bar. The reaction was started by increasing temperature from 180° to the reaction temperature. The gaseous reaction products were analyzed online by gas chromatography (GC Varian 3800). Analysis of H_2, CO, CO_2, CH_4, and N_2 was performed using a CTR-1 column. Hydrocarbons (C_1−C_7) were separated in a capillary CP-Plot column. Carbon monoxide contained 5% nitrogen which was used as an internal standard. The selectivity was calculated on carbon basis. The catalyst samples were transferred from the reactor to the analysis chamber of the STEM-EELS microscope without exposure to air. After the FT catalytic test, the reactor was cooled to room temperature, isolated with the valves from the gas manifold and transferred to Jacomex GP Campus glovebox (Ar atmosphere, O_2 concentration <0.1 ppm). In the glovebox, the catalyst was discharged from the reactor to a 5 mL vial filled with heptane. Then the vial was kept in a hermetically sealed bottle filled with argon. Prior to STEM-EELS analysis, the vial was open in an oxygen-free glovebag attached to the analysis chamber of STEM-EELS microscope. In the glovebox, the sample was removed from the vial, set on the grid, and transferred to the analysis chamber without any exposure to air.

The STEM- EELS experiments were performed at the Laboratory of Solid State Physics at Orsay using a 100 keV STEM microscope (VG HB 501) spectrometer equipped with a cold field emission source (CFEG). The EEL spectra were recorded with a charge-coupled device (CCD) camera optically coupled to a scintillator in the image plane of a Gatan 666 parallel EELS spectrometer. The high brightness CFEG source allows the formation of small probes (∼0.5 nm) and an energy resolution close to 0.5 eV on core losses. The EELS data were acquired in the Spectrum Imaging Mode[38] by scanning the probe over a region of interest while acquiring a whole EELS spectrum in parallel with the HAADF signal at each probe position. The elemental maps were obtained from typical sets of 32 × 32 spectra plotting the characteristic signal over a given energy range after background removal.

RESULTS AND DISCUSSION

The BET surface area of the calcined $CoPt/Al_2O_3$ catalyst was 160 m^2/g, while the average pore diameter was 8 nm. In addition to γ-Al_2O_3, the calcined catalyst contained Co_3O_4 nanoparticles of 9 nm measured from XRD Scherrer broadening. The catalyst characterization data were consistent with previous reports.[11,37] Previously,[11] TEM showed the cobalt oxide particle size distribution in this $CoPt/Al_2O_3$ catalyst between 4 and 15 nm. To evaluate the impact of FT reaction

dx.doi.org/10.1021/cs500981p | ACS Catal. 2014, 4, 4510−4515

Table 1. Activation, Reaction Conditions (P = 20 bar, H_2/CO = 2) and Catalytic Performance of the Catalyst Samples Used for STEM-EELS Analysis

test	T, °C	GHSV, $cm^3\ g^{-1}\ h^{-1}$	X_{CO}, %	cobalt time yield, $mol_{CO}\ mol_{Co}^{-1}\ s^{-1}$	S_{CH4}, %	S_{CO2}, %	S_{C5+}, %	comments
catalyst reduction	400	2000	-	-	-	-	-	catalyst activation for Tests I, II, and III
Test I (standard conditions)	220	6000	69.9	3.81	8.6	0.5	84.0	test under standard conditions
Test II (long-term severe conditions)	240 (5 h)	12 000	72	7.85	13.1	3.1	82.3	long-term test under severe FT conditions
	240 (170 h)	12 000	58.8	6.41	12.8	0.6	77.8	
Test III (with excursion to high temperature)	220	6000	67.9	3.70	8.9	0.7	86.6	test under standard conditions
	340	6 000	100.0	5.45	99	0.2	<1.0	excursion to higher temperatures (340 °C)
	220	6000	29.9	1.63	26.5	0.6	54.6	return to 220 °C

conditions on the catalyst structure and possible oxidation of cobalt nanoparticles, four catalyst samples were prepared for STEM-EELS analysis (Table 1):

- $CoPt/Al_2O_3$−R reduced sample,
- $CoPt/Al_2O_3$−I catalyst exposed to standard conditions of FT synthesis for 20 h,
- $CoPt/Al_2O_3$−II catalyst treated in syngas at 240 °C for 170 h,
- $CoPt/Al_2O_3$−III catalyst after excursion in syngas to 340 °C.

For STEM-EELS analysis, in order to avoid possible cobalt oxidation, all samples were transferred from the catalytic reactor to the analysis chamber of STEM VG HB 501 microscope without any exposure to air.

Reduced Catalyst ($CoPt/Al_2O_3$−R). Reduction in hydrogen is a most common procedure for activation of cobalt FT catalysts. It converts cobalt oxide nanoparticles into cobalt metallic species which contain active sites for FT synthesis. In this work, the catalyst was activated in a flow of hydrogen at 400 °C. The reduction temperature was chosen on the basis of previously conducted TPR and in situ XANES experiments.[11,25] Those experiments were indicative of complete cobalt reduction in this Pt-promoted cobalt catalyst in H_2 at 400 °C. Figure S1, Supporting Information (SI), shows cobalt and oxygen elemental maps for the $CoPt/Al_2O_3$−R catalyst. The reduced catalyst showed the presence of only metallic cobalt particles of 7−15 nm. Cobalt L_2 and L_3 edges peaks (in the 778−790 eV energy range) and oxygen K-edge (onset at about 532 eV) were observed in the EELS spectrum. Analysis of K-edge of oxygen in the $CoPt/Al_2O_3$−R sample did not reveal the presence of the oxygen K pre-edge feature characteristic of cobalt oxides (Figure S2, SI). All detected oxygen atoms seem to be related to alumina. This suggests that concentration of cobalt oxide is negligible in this sample. This observation is also consistent with very high extent of cobalt reduction in hydrogen at 400 °C in cobalt catalyst promoted with platinum.[11] It is well-known[1,2,11,16,17,39,40] that promotion of supported cobalt catalysts with noble metals results in a remarkable enhancement of cobalt reducibility. The conducted experiment also validates the procedure used for sample transfer from the catalytic reactor to STEM-EELS analysis chamber. Notably, no bulk or surface cobalt oxidation occurs during the sample handling and transfer.

Catalyst after Standard FT Test at 220 °C ($CoPt/Al_2O_3$−I). In the second experiment, the reduced catalyst was exposed to standard conditions of low temperature FT synthesis. After reduction in hydrogen at 400 °C, the catalyst was exposed to syngas at 180 °C, and the temperature was linearly increased to 220 °C. No visible heat transfer problem was observed in the millifixed bed reactor during this temperature ramp. Table 1 displays the catalytic performance data for $CoPt/Al_2O_3$ obtained in Test I. The catalyst has shown high liquid hydrocarbon and wax productivities. Carbon monoxide conversion, methane, C_{5+} and CO_2 selectivities measured at 220 °C, P = 20 bar and H_2/CO = 2 were consistent with previous results[2,8,11] for similar catalysts. A slow catalyst deactivation was observed (see Figure S3, SI). After Test I, the reactor was cooled to room temperature. Figure 1 displays cobalt and oxygen elemental maps and intensity profiles for the used $CoPt/Al_2O_3$−I catalyst. Cobalt metallic particles in the range between 7 and 15 nm were detected. The observed cobalt particle size is consistent with our previous operando experiments[11,25] and literature data.[8] To identify possible presence of cobalt oxide species after Test I, the spatially resolved EELS spectra were measured at the center and at the edges of cobalt metal particles (Figure 1d). The EELS spectra were rather similar to those observed for the reduced $CoPt/Al_2O_3$−R sample. In both cases, no oxygen K

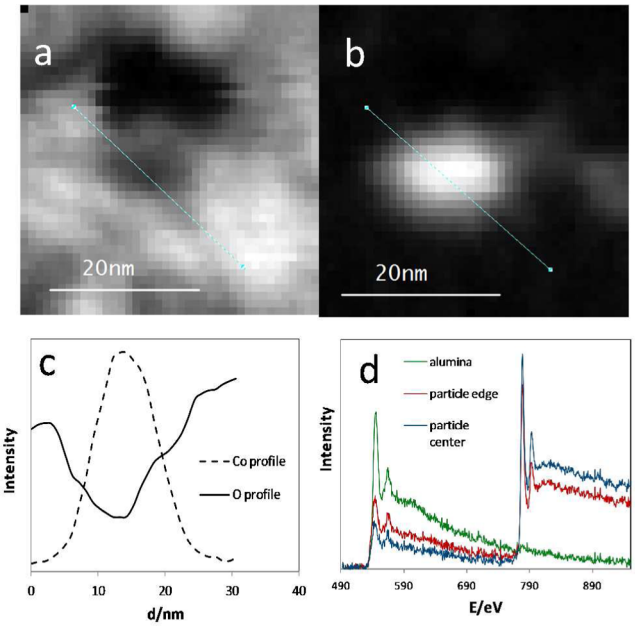

Figure 1. Oxygen (a), cobalt elemental (b) maps, cobalt and oxygen profiles in a selected cobalt nanoparticle (c), EELS measured in alumina, cobalt particle edge and particle center (d) in $CoPt/Al_2O_3$−I.

dx.doi.org/10.1021/cs500981p | ACS Catal. 2014, 4, 4510−4515

pre-edge feature was observed. Moreover, the oxygen intensity map shows a monotonous decay down from the edges to the center of the particle. In agreement with previous results,[8,11,23,25] STEM-EELS data suggests the absence of cobalt surface or bulk oxidation in the alumina-supported cobalt catalyst after standard Test I. Some decrease in the FT reaction rate observed in Test I can be therefore attributed to other deactivation phenomena.

Catalyst after Long-Term FT Test at 240 °C ($CoPt/Al_2O_3$–II). To evaluate the effect of catalyst deactivation in a longer test under more severe conditions of FT synthesis, the catalyst was exposed to syngas at 240 °C for 170 h at a 2-fold higher GHSV (Test II, Table 1). The increase in reaction temperatures led to a higher cobalt time yield, higher methane, and lower C_{5+} selectivity compared to Test I conducted at 220 °C. The catalyst exhibited a noticeable deactivation (Figure S4, SI); the cobalt time yield decreased from 7.85 to 6.41 $mmol_{CO}$ mol_{Co}^{-1} s^{-1} after 170 h on stream. A slight decrease in C_{5+} selectivity was also observed.

Cobalt, oxygen elemental maps and intensity profiles in $CoPt/Al_2O_3$–II are shown in Figure S5, SI. They indicate the presence of cobalt metal nanoparticles with diameter comparable to that of $CoPt/Al_2O_3$–R and $CoPt/Al_2O_3$–I. The oxygen profile curve (Figure S5c) shows a small peak at the edge of cobalt metal nanoparticle. A careful analysis of space resolved cobalt and oxygen STEM-EELS data of $CoPt/Al_2O_3$–II showed the presence of oxygen K pre-edge feature at the edge of cobalt metal nanoparticles (Figure S 5d). Both observations could be indicative of the presence of cobalt oxide species in the interface between cobalt nanoparticle and alumina. These species can be produced by surface oxidation of cobalt during FT reaction at more severe reaction conditions (240 °C, time-on-stream 170 h).

Catalyst after Excursion in Syngas to 340 °C ($CoPt/Al_2O_3$–III). Insufficient heat transfer is a serious problem in FT synthesis. Heat transfer limitations could lead to hot spots, temperature gradients and even to reactor runaway, when the reactor temperature uncontrollably increases[37] to very high values. In order to simulate the FT reactor runaway and to investigate the influence of high temperature on the catalyst structure, the temperature of the millifixed bed reactor was intentionally increased from 220 to 340 °C and kept at this temperature for 72 h. The experimental procedure and catalytic data are presented in Table 1 (Test III). At 340 °C and GHSV = 6000 cm^3 g^{-1} h^{-1}, carbon monoxide conversion was close to 100% during the whole duration of the test. Methane selectivity increased from 8.9 to 99%. After 48 h at 340 °C, the reactor temperature again was decreased to 220 °C. The catalyst was strongly deactivated, the cobalt time yield decreased about 2 times to 1.63 $mmol_{CO}$ mol_{Co}^{-1} s^{-1} in comparison with the same catalyst before excursion to high temperature (3.73 $mmol_{CO}$ mol_{Co}^{-1} s^{-1}). A much higher methane selectivity was observed (Table 1). After having completed Test III, the catalyst was transferred without exposure to air to STEM-EELS analysis chamber. Representative Co and O maps are shown in Figure 2. Interestingly, after excursion to 340 °C much larger cobalt particles (>20–30 nm) were detected in the catalyst. This indicates cobalt sintering which might occur at high temperature. In agreement with previous reports,[27,41,42] cobalt sintering could be facilitated by the presence of larger water amounts at higher carbon monoxide conversion. Differently to iron, cobalt catalysts are not very active in water gas shift reaction: $CO+H_2O=CO_2+H_2$. Indeed, very small amounts of

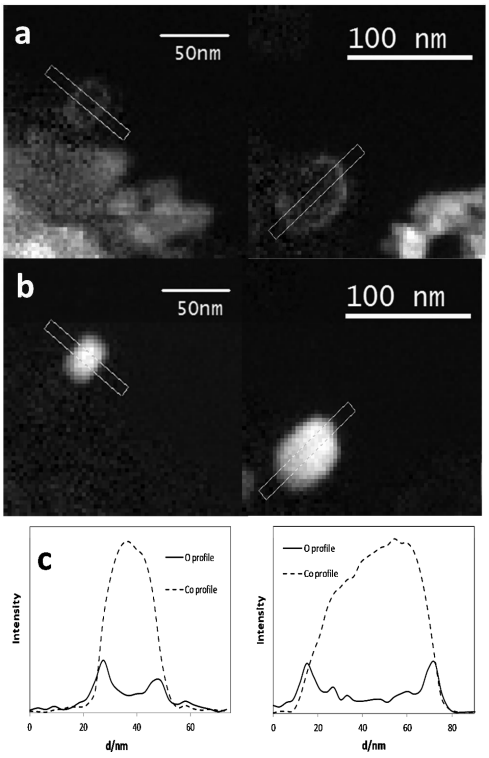

Figure 2. STEM-EELS data for the $CoPt/Al_2O_3$–III after excursion to 340 °C: (a) oxygen map, (b) cobalt map, (c) oxygen and cobalt profiles in selected cobalt nanoparticles.

carbon dioxide are produced (Table 1). This suggests that significant amounts of water are present in the catalyst at higher carbon monoxide conversion levels.

The most exciting feature however relates to the presence of very distinct oxygen halos around cobalt metal particles (Figure 2a). In addition, this halo is also visible in the oxygen intensity profile (Figure 2c). The halos around cobalt metal nanoparticles are associated with the pre-edge K oxygen features in EELS at the cobalt nanoparticle edges (Figure S6, SI). This suggests that these halos cannot be due to the oxygen atoms of alumina[30,36] but should be assigned to CoO_x species. These CoO_x species represent cobalt oxide layer on the surface on cobalt metal nanoparticles. Some contribution of surface cobalt aluminate to this layer cannot be completely ruled out. The particle morphology (metal particles clearly distinguishable from the support) is more indicative, however, of the presence of surface cobalt oxides rather than of Co–Al species.

Note that no oxygen halo around cobalt metallic particles was observed in the reduced $CoPt/Al_2O_3$–R sample (Figure S1, SI) or in the $CoPt/Al_2O_3$–I catalyst exposed to syngas under standard conditions of FT synthesis (Figure 1). This halo was hardly detected in $CoPt/Al_2O_3$–II exposed to FT synthesis at 240 °C (Figure S5, SI). In that sample, the presence of CoO_x species in the shell of cobalt nanoparticles was uncovered from the oxygen K pre-edge feature (Figure S 5d).

Thus, the STEM-EELS results clearly indicate surface oxidation of cobalt particles in FT reaction. Note that even in the particles containing the cobalt oxide shell, the particle core remains metallic and was not affected by oxidation. The surface oxidation takes place in the presence of larger concentrations of water produced by FT reaction and low pressures of hydrogen, which are characteristic of higher carbon monoxide conversions (~100%). Surface oxidation of cobalt nanoparticles during FT

dx.doi.org/10.1021/cs500981p | ACS Catal. 2014, 4, 4510–4515

synthesis by water is consistent with recently performed thermodynamic calculations.[27] Formation of surface cobalt oxide monolayer is thermodynamically favorable because it results in lower surface energy of cobalt nanoparticles. The formation of surface cobalt oxide layer also results in a decrease in the concentration of cobalt active sites and lower activity in FT synthesis. Indeed, significant deactivation with time on-stream was observed on $CoPt/Al_2O_3$–II and $CoPt/Al_2O_3$–III, which showed surface oxidation of cobalt nanoparticles (Table 1). Cobalt surface oxidation results in higher methane selectivity. This observation is consistent with recent reports,[19−21] which showed a major increase in methane selectivity on partially oxidized cobalt catalysts. Note that the coverage of cobalt nanoparticles by oxide species could be incomplete and some of cobalt metal sites could be still available for the reaction.

CONCLUSION

This paper provides the first direct experimental evidence of surface oxidation of cobalt metal nanoparticles in supported catalysts during FT synthesis. Formation of cobalt oxide shell on the surface of cobalt metallic nanoparticles occurs under high carbon monoxide conversions and is favored by higher reaction temperature. This surface oxidation could be a major reason for catalyst deactivation at higher reaction temperatures. This phenomenon may coincide with the formation of hot spots in the catalyst at the beginning of the reaction and can be accompanied by other deactivation processes.

ASSOCIATED CONTENT

Supporting Information

The following file is available free of charge on the ACS Publications website at DOI: 10.1021/cs500981p.

Cobalt, oxygen maps, intensity profiles and EELS spectra at oxygen K-edge in the $CoPt/Al_2O_3$–R and $CoPt/Al_2O_3$–II; carbon monoxide conversion as a function of time on stream in Tests I and II; EELS spectra of $CoPt/Al_2O_3$–III (PDF).

AUTHOR INFORMATION

Corresponding Author

*E-mail: andrei.khodakov@univ-lille1.fr. Tel.:+33 3 20 33 54 39. Fax: +33 3 20 43 65 61.

Present Address

‖(for P.F.) Université Lyon 1, CNRS, UMR 5256, IRCELYON, Institut de recherches sur la catalyze et l'environnement de Lyon, 2 avenue Albert Einstein, 69626 Villeurbanne, France.

Notes

The authors declare no competing financial interest.

ACKNOWLEDGMENTS

C.L. and O.S. thank Alexandre Gloter for his help in interpreting the Co L and O K signals. The authors acknowledge financial support from the CNRS-CEA "METSA" microscopy French network for the STEM-EELS experiments. The authors thank Total S.A. for financial support of this work.

REFERENCES

(1) Melaet, G.; Ralston, W. T.; Li, C. S.; Alayoglu, S.; An, K.; Musselwhite, N.; Kalkan, B.; Somorjai, G. A. *J. Am. Chem. Soc.* **2014**, *136*, 2260−2263.

(2) *Handbook of Heterogeneous Catalysis*; Ertl, G., Knözinger, H., Schüth, F., Weitkamp, J., Eds.; Wiley-VCH: Weinheim, Germany, 2008; Vol.6.

(3) Bell, A. T. *Nature* **2008**, *456*, 185−186.

(4) Dry, M. E. *Catal. Today* **2002**, *71*, 227−241.

(5) Khodakov, A. Y.; Chu, W.; Fongarland, P. *Chem. Rev.* **2007**, *107*, 1692−1744.

(6) Bezemer, G. L.; Bitter, J. H.; Kuipers, H. P. C. E.; Oosterbeek, H.; Holewijn, J. E.; Xu, X.; Kapteijn, F.; van Dillen, A. J.; de Jong, K. P. *J. Am. Chem. Soc.* **2006**, *128*, 3956−3964.

(7) Høydalsvik, K.; Fløystad, J. B.; Voronov, A.; Voss, G. J. B.; Esmaeili, M.; Kehres, J.; Granlund, H.; Vainio, U.; Andreasen, J. W.; Rønning, M.; Breiby, D. W. *J. Phys. Chem. C* **2014**, *118*, 2399−2407.

(8) Saib, A. M.; Moodley, D. J.; Ciobîc, I. M.; Hauman, M. M.; Sigwebela, B. H.; Weststrate, C. J.; Niemantsverdriet, J. M.; van De Loosdrecht, J. *Catal. Today* **2010**, *154*, 271−282.

(9) Tsakoumis, N. E.; Rønning, M.; Borg, Ø.; Rytter, E.; Holmen, A. *Catal. Today* **2010**, *154*, 162−182.

(10) Peña, D.; Griboval-Constant, A.; Diehl, F.; Lecocq, V.; Khodakov, A. Y. *ChemCatChem* **2013**, *5*, 728−731.

(11) Karaca, H.; Safonova, O. V.; Chambrey, S.; Fongarland, P.; Roussel, P.; Griboval-Constant, A.; Lacroix, M.; Khodakov, A. Y. *J. Catal.* **2011**, *277*, 14−26.

(12) Moodley, D. J.; van de Loosdrecht, J.; Saib, A. M.; Overett, M. J.; Datye, A. K.; Niemantsverdriet, J. W. *Appl. Catal., A* **2009**, *354*, 102−110.

(13) Peña, D.; Griboval-Constant, A.; Lecocq, V.; Diehl, F.; Khodakov, A. Y. *Catal. Today* **2013**, *215*, 43−51.

(14) Peña, D.; Griboval-Constant, A.; Lancelot, C.; Quijada, M.; Visez, N.; Stéphan, O.; Lecocq, V.; Diehl, F.; Khodakov, A. Y. *Catal. Today* **2014**, *228*, 65−76.

(15) Jacobs, G.; Patterson, P. M.; Das, T. K.; Luo, M.; Davis, B. H. *Appl. Catal.,A* **2004**, *270*, 65−76.

(16) Jacobs, G.; Ma, W.; Davis, B. H. *Catalysts* **2014**, *4*, 49−76.

(17) Jacobs, G.; Ma, W.; Gao, P.; Todic, B.; Bhatelia, T.; Bukur, D. B.; Davis, B. H. *Catal. Today* **2013**, *214*, 100−139.

(18) Huffman, G. P.; Shah, N.; Zhao, J. M.; Huggins, F. E.; Hoost, T. E.; Halvorsen, S.; Goodwin, J. G. *J. Catal.* **1995**, *151*, 17−25.

(19) Ma, W.; Jacobs, G.; Ji, Y.; Bhatelia, T.; Bukur, D.; Khalid, S.; Davis, B. H. *Top. Catal.* **2011**, *54*, 757−767.

(20) Azzam, K.; Jacobs, G.; Ma, W.; Davis, B. H. *Catal. Lett.* **2014**, *144*, 389−394.

(21) Jermwongratanachai, T.; Jacobs, G.; Shafer, W. D.; Ma, W.; Pendyala, V. R. R.; Davis, B. H.; Kitiyanan, B.; Khalid, S.; Cronauer, D. C.; Kropf, A. J.; Marshall, C. L. *Top. Catal.* **2014**, *57*, 479−490.

(22) van Steen, E.; Claeys, M.; Dry, M. E.; van DeLoosdrecht, J.; Viljoen, E. L.; Visagie, J. L. *J. Phys. Chem. B* **2005**, *109*, 3575−3577.

(23) Saib, A. M.; Borgna, A.; van de Loosdrecht, J.; van Berge, P. J.; Niemantsverdriet, J. W. *Appl. Catal., A* **2006**, *312*, 12−19.

(24) Rochet, A.; Moizan, V.; Pichon, C.; Diehl, F.; Berliet, A.; Briois, V. *Catal. Today* **2011**, *171*, 186−191.

(25) Sadeqzadeh, M.; Karaca, H.; Safonova, O. V.; Fongarland, P.; Chambrey, S.; Roussel, P.; Griboval-Constant, A.; Lacroix, M.; Curulla-Ferré, D.; Luck, F.; Khodakov, A. Y. *Catal. Today* **2011**, *164*, 62−67.

(26) Fischer, N.; Clapham, B.; Feltes, T.; van Steen, E.; Claeys, M. *Angew. Chem.* **2014**, *126*, 1366−1369.

(27) Sadeqzadeh, M.; Chambrey, S.; Hong, J.; Fongarland, P.; Luck, F.; Curulla-Ferré, D.; Schweich, D.; Bousquet, J.; Khodakov, A. Y. *Ind. Eng. Chem. Res.* **2014**, *53*, 6913−6922.

(28) Hitchcock, A. P.; Dynes, J. J.; Johansson, G.; Wang, J.; Botton, G. *Micron* **2008**, *39*, 741−748.

(29) Bezemer, G. L.; Radstake, P. B.; Falke, U.; Oosterbeek, H.; Kuipers, H. P. C. E.; van Dillen, A. J.; de Jong, K. P. *J. Catal.* **2006**, *237*, 152−161.

(30) Shannon, M. D.; Lok, C. M.; Casci, J. L. *J. Catal.* **2007**, *249*, 41−51.

(31) Jacobs, G.; Sarkar, A.; Ji, Y.; Luo, M.; Dozier, A.; Davis, B. H. *Ind. Eng. Chem. Res.* **2008**, *47*, 672−680.

(32) Morales, F.; Grandjean, D.; de Groot, F. M. F.; Stephan, O.; Weckhuysen, B. M. *Phys. Chem. Phys.Chem.* **2005**, *7*, 568−572.
(33) Morales, F.; de Groot, F. M.F.; Gijzeman, O. L.J.; Mens, A.; Stephan, O.; Weckhuysen, B. M. *J. Catal.* **2005**, *230*, 301−308.
(34) Wang, Z. I.; Bentley, J.; Evans, N. B. *Micron* **2000**, *31*, 355−362.
(35) Wang, Z. I.; Sin, J. S.; Jiang, Y. D. *Micron* **2000**, *31*, 571−580.
(36) Li, P.; Liu, J.; Nag, N.; Crozier, P. A. *Appl. Catal., A* **2006**, *307*, 212−221.
(37) Chambrey, S.; Fongarland, P.; Karaca, H.; Piché, S.; Griboval-Constant, A.; Schweich, S.; Luck, F.; Savin, S.; Khodakov, A. Y. *Catal. Today* **2011**, *171*, 201−206.
(38) Colliex, C.; Tencé, M.; Lefévre, E.; Mory, C.; Gu, H.; Bouchet, D.; Jeanguillaume, C. *Microchimica Acta* **1994**, *114−115*, 71−87.
(39) Jacobs, G.; Das, T. K.; Zhang, Y.; Li, J.; Racoillet, G.; Davis, B. H. *Appl. Catal., A* **2002**, *233*, 263−281.
(40) Tsubaki, N.; Sun, S.; Fujimoto, K. *J. Catal.* **2001**, *199*, 236−246.
(41) Bezemer, G. L.; Remans, T. J.; van Bavel, A. P.; Dugulan, A. I. *J. Am. Chem. Soc.* **2010**, *132*, 8540−8541.
(42) Sadeqzadeh, M.; Hong, J.; Fongarland, P.; Curulla-Ferré, D.; Luck, F.; Bousquet, J.; Schweich, D.; Khodakov, A. Y. *Ind. Eng. Chem.Res.* **2012**, *51*, 11955−11964.